The CSU Tethered Balloon Data Set of the FIRE Marine Stratocumulus IFO

by
Paul F. Hein, Stephen K. Cox, Wayne H. Schubert, Christopher M. Johnson-Pasqua, David P. Duda, Thomas A. Guinn, Mike Mulloy, Thomas B. McKee, William L. Smith Jr., and John D. Kleist

Department of Atmospheric Science
Colorado State University
Fort Collins, Colorado

Funding: NASA Office of Naval Research
FIRE series No. 6

Colorado State University

Department of Atmospheric Science

Paper No. 432

THE CSU TETHERED BALLOON DATA SET OF THE FIRE MARINE STRATOCUMULUS IFO

FIRE Series No. 6

by

Paul F. Hein

Stephen K. Cox

Wayne H. Schubert

Christopher M. Johnson-Pasqua

David P. Duda

Thomas A. Guinn

Mike Mulloy

Thomas B. McKee

William L. Smith, Jr.

John D. Kleist

November, 1988

Atmospheric Science Paper No. 432

ACKNOWLEDGEMENTS

This research was funded by ONR under grant N00014-87-K-0228/P00001 and by NASA under grant NAG 1-554.

CONTENTS

LIST OF TABLES

LIST OF FIGURES

Chapter 1

INTRODUCTION

This paper provides a description of the Colorado State University (CSU) instrumentation and data collected during the Marine Stratocumulus Intensive Field Observations (MStCu IFO) of the First ISCCP (International Satellite Cloud Climate Program) Regional Experiment (FIRE).

The MStCu IFO was conducted off the California coast at and in the vicinity of San Nicolas Island from 29 June 1987 to 20 July 1987. The MStCu IFO was a coordinated effort utilizing five aircraft, satellite observations, and surface sites. Surface instrumentation was located at the northwest tip of the island, well exposed to the prevailing northwesterly boundary layer winds. Instrumentation deployed at San Nicolas Island included two tethered balloon instrument packages, an instrumented tower, a microwave radiometer, a doppler radar, a doppler sodar, radiometric instrumentation, a sea state sensor, a laser ceilometer, and rawinsondes. These instruments measured fluxes (including radiation flux), up and down radiances, cloud microphysics, aerosols, liquid water profiles, sea state, cloud height, vertical winds, and the basic meteorological variables (temperature, humidity, wind, etc).

Chapter 2 contains a brief description of the instruments in the tethered balloon package, the surface station, and the rawinsonde station. In Chapter 3, the available data sets are described. Appendix A contains a summary of the tethered balloon flights and a brief list of instrument problems. A summary of the CLASS rawinsonde flights is found in Appendix B with a data quality rating for each flight.

Chapter 2

INSTRUMENTATION

2.1 CSU Tethered Balloon Package

The CSU tethered balloon package, shown in Figure 2.1, contained instruments that measured pressure, temperature, humidity, wind, radiation, and cloud droplet size. (Beneath the CSU platform, the British Meteorology Office, BMO, deployed several fast response instrument packages that attached at various heights on the cable. The BMO instruments measured temperature, humidity, and the u, v and w components of the wind with a 20 Hz sampling frequency to measure the turbulent fluxes.)

2.1.1 Pressure

The pressure was measured by a digiquartz pressure transducer, which accurately compensated for the effects of temperature. The transducer has a range from 0 to 1034.21 mb with a repeatability of $\pm 0.005\%$ of the full scale and a hystersis of $\pm 0.005\%$ of the full scale.

2.1.2 Wet and Dry Bulb Temperatures

The wet and dry bulb temperatures were measured by a Cu-Cn thermocouple psychrometer. The instrument has a temperature range from -20° to 80°C with a resolution of ± 0.008°C. A thermistor psychrometer was also aboard. The temperature range of the thermistor psychrometer is from 0 to 40°C with a resolution of ± 0.1°C. The psychrometers are seen in Figure 2.2, positioned at the front of the platform beneath the wind vane.

2.1.3 Wind Speed and Direction

The wind was measured with the Wind Monitor Model 05103 by the R.M. Young Company, which consists of a four blade propeller mounted on a wind vane (Fig. 2.2).

The propeller has a distance constant of 3.3 m and a threshold sensitivity of 0.7 m/s. Wind speeds between 0 and 60 m/s can be measured. The vane assembly has a threshold sensitivity of 1.0 m/s and a damping ratio of 0.23. The vane measures wind direction relative to the platform from -177.5° to 177.5° with a 5° dead gap. Because the platform was not stationary, a compass was needed along with the vane to find the wind direction. Two Air Inc. latching compasses were aboard. The compasses have a range from -180 to 180° with an accuracy of ±5.0°. Each compass has a dead region of a couple of degrees. The dead region of one compass faced to the back of the platform and the other to the left side (when facing toward the platform front) 90° rotated from the back.

2.1.4 Radiation

The upwelling and downwelling shortwave radiation was measured by four Eppley pyranometers. Two pyranometers measured irradiance in a spectral bandpass from 0.3 to 2.8 μm and the other two with dark red Schott filter glass domes measured wavelengths from 0.7 to 2.8 μm. Figure 2.3 shows the two upward looking pyranometers on the platform. The sensitivity of these instruments is nominally 9 microvolts/(W/m^2) with an impedance of 650 ohms. The temperature dependence of the instrument is ±1 % over an ambient temperature range from -20° to 40°C. The response time of the pyranometers is 1 second.

The upwelling and downwelling longwave irradiance, 4 to 50 μm, was measured with two Eppley pyrgeometers (Fig. 2.4). These instruments typically have a sensitivity of 5 microvolts/(W/m^2) and an impedance of 700 ohms. Temperature effects cause errors of ±2 % over a temperature range of -20° to 40°C. The response time of the pyrgeometers is 2 seconds.

The Bugeye, CSU Multidirectional Photodiode Radiometer, (Davis, *et al.*, 1982) measures spatial and temporal variations in radiance patterns. It consists of a hemispherical array of thirteen silicon photodiodes and associated electrical circuitry mounted on an aluminum housing. There were two bugeyes on the platform, one looking up and the other looking down. Figure 2.3 shows the upward looking bugeye. The upward looking

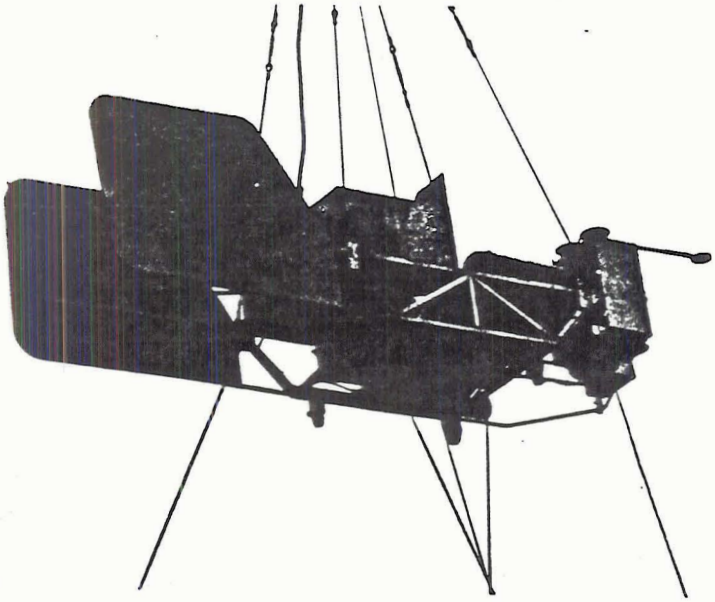

Figure 2.1: Deployed CSU tethered balloon package.

Figure 2.2: The balloon platform wind vane and propeller and the psychrometers beneath the vane.

bugeye had diodes with a 10° field of view that were configured as shown in Table 2.1. The diodes on the downward looking bugeye were configured as described in Table 2.2. Each diode of the downward looking bugeye had a 50° field of view. The bugeyes have a range of 360 to 1100 nm using a minimum sensitivity of .01 amps/watt. The diodes of the downward looking bugeye are covered with a blue tinted Schott glass filters. The spectral response of the downward looking bugeye is shown in Figure 2.4. The peak sensitivity of the downward looking bugeye is .14 amps/watt at 400 nm. The spectral response of the upward looking bugeye is shown in Figure 2.5, and the peak sensitivity of the upward looking bugeye is about .50 amps/watt at 925 nm.

2.1.5 Cloud Microphysics

The Particle Measuring System Forward Scattering Spectrometer Probe (FSSP) is an instrument designed to measure the in situ particle size. Particles passing through the FSSP sampling volume will scatter a focused laser beam into the optics aperture where the scattered light measured. The amount of scattered light indicates the size of the particle. The FSSP is shown in Figure 2.6. Particles from 0.5 μm to 47 μm can be measured with a size resolution as fine as 0.5 μm. (At the bottom of Table 3.3, the size ranges available are listed.) It will operate between -40° and 40°C, from 0 to 40,000 feet, and from 0 to 100% relative humidity. The FSSP on the platform relied on the ambient wind to propel the cloud droplets through the FSSP sampling volume.

2.1.6 Platform Orientation

Pitch and roll of the platform were measured with a Sperry Electronic Clinometer. This is an angle measurement system. The total range is from -60° to 60°, and the linear range is between -45° and 45°. Threshold and resolution are .001°, and the operating range is from -40° to 65°C. The time constant is 0.3 seconds and the frequency response is 1.0 Hz.

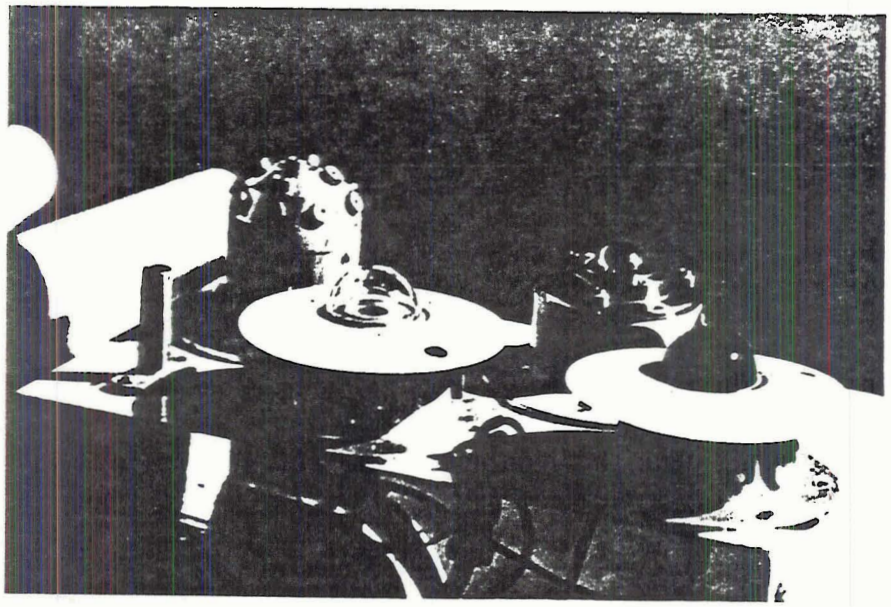

Figure 2.3: The balloon platform upward looking radiometric instrumentation: two pyranometers, a pyrgeometer, and a bugeye.

Table 2.1: The angular positions of the upward looking bugeye photodiodes. (Azimuth angle of zero degrees is forward looking and the angles increase in value in the clockwise direction as one faces the bugeye dome.)

Detector Number	Zenith Angle (degrees)	Azimuth Angle (degrees)
1	0	—
2	30	180
3	30	90
4	30	0
5	30	270
6	60	180
7	60	135
8	60	90
9	60	45
10	60	0
11	60	315
12	60	270
13	60	225

Table 2.2: The angular positions of the downward looking bugeye photodiodes. (Azimuth angle of zero degrees is forward looking and the angles increase in value in the clockwise direction as one faces the bugeye dome.)

Detector Number	Zenith Angle (degrees)	Azimuth Angle (degrees)
1	0	—
2	30	330
3	30	90
4	30	210
5	45	30
6	45	150
7	45	270
8	60	0
9	60	60
10	60	120
11	60	180
12	60	240
13	60	300

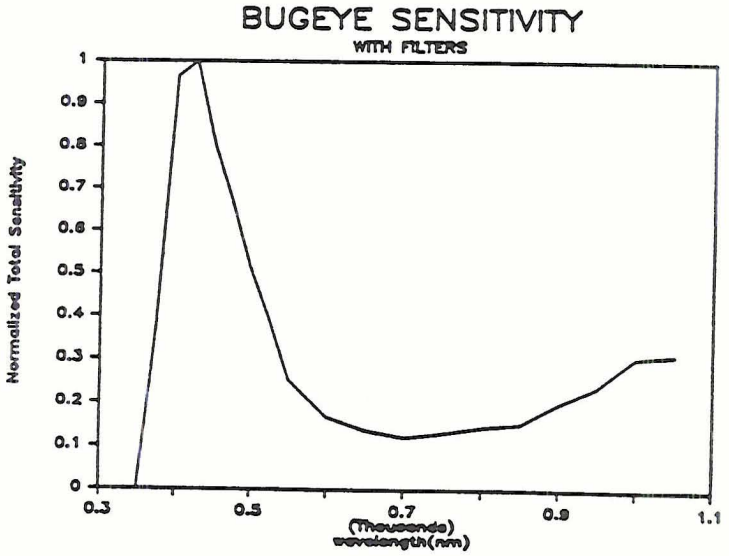

Figure 2.4: Spectral response of downward looking bugeye.

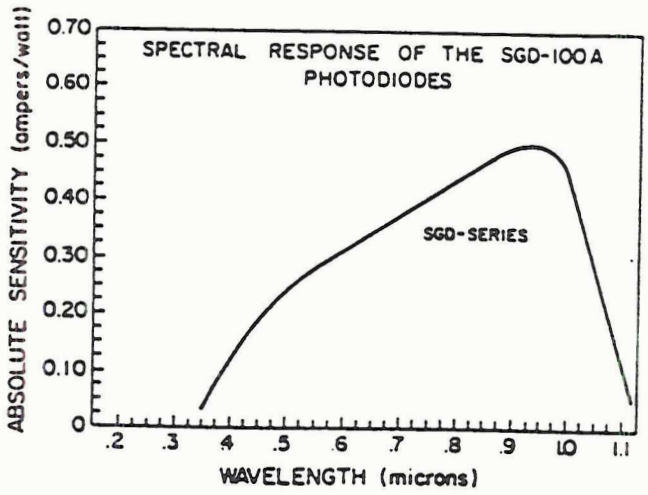

Figure 2.5: Spectral response of upward looking bugeye.

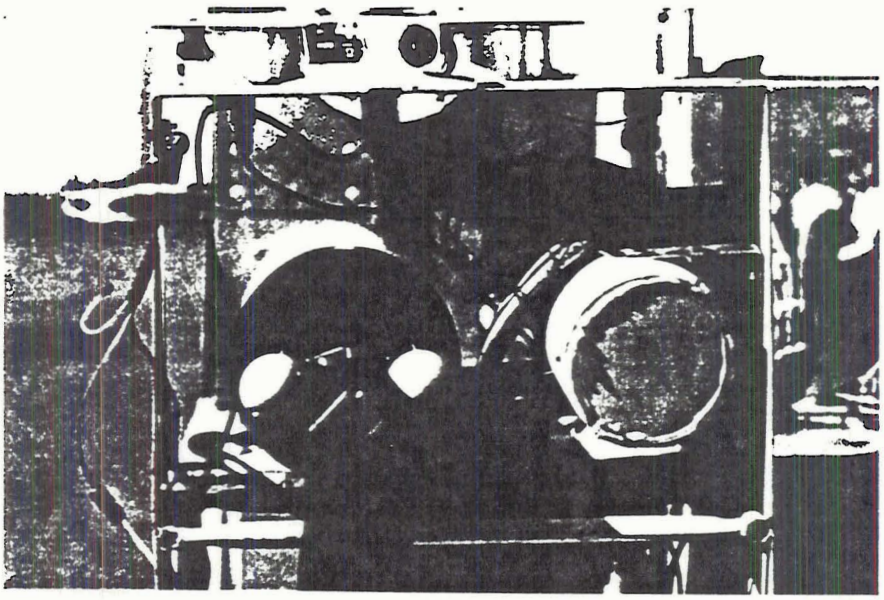

Figure 2.6: The balloon platform FSSP.

2.1.7 Video Imagery

Images of the upwind sky conditions were obtained by using a video camera and video cassette recorder. The camera operated for 10 seconds and was off for next 10 seconds before repeating this cycle. The time and date were encoded on each frame.

2.2 Surface Instrumentation

The ground-based CSU instruments measured temperature, humidity, wind, radiation, and cloud base height. Visual conditions were preserved with photographs that are taken by a 35 mm camera with the date encoded on each frame.

2.2.1 Wet and Dry Bulb Temperatures

The air temperature and the dew point temperature were obtained by a Campbell Scientific Model 207 containing a Phys-Chemical Research PCRC-11 RH sensor and a Fenwal Electronics UUT 51J1 thermistor configured with a Campbell Scientific CR7 datalogger. The error is generally less than $\pm 0.2°C$ over the temperature range -33° to +48°C. However, in a worst case example all of the errors could add up to yield a $\pm 0.4°C$ accuracy.

2.2.2 Wind Speed and Direction

Wind speed was sensed by a model O14A Met-One Wind Speed Sensor from Campbell Scientific Inc. It consists a three cup anemometer assembly and a magnet read switch assembly to produce a series of contact closures whose frequency is proportional to wind speed. The maximum operating range is 0–60 m/s with a starting speed of 0.5 m/s. The calibrated range is from 0–50 m/s. The anemometer has an accuracy of $\pm 1.5\%$ and an operational temperature range from -50° to 85°C. The distance constant of the anemometer is less than 15 feet.

Wind direction was obtained by using a Met One O24A wind direction sensor. The sensor uses a light weight air-foil vane and a potentiometer which will produce an output that is proportional to the wind direction. The vane measured the wind direction from 0° to 356° with a dead gap from 357° to 360°. The threshold is 1.0 mph, and the accuracy is $\pm 5°$. The standard damping ratio is 0.25. The delay distance is less than 5 feet. The instrument will operate between -50° and 70°C.

2.2.3 Radiation

The shortwave and longwave radiation measurements were performed by two upward looking Eppley pyranometers and an upward looking Eppley pyrgeometer with the same characteristics as those aboard the tethered balloon platform. There was also a multi-field of view radiometer (MFOV) at the site. The MFOV uses 5 silicon photodiodes aligned along a common optical axis. Each photodiode is at the end of a collimator tube. Each tube is a different length to provide five different fields of view (2, 5, 10, 20 and 28°). The instrument is mounted on a LI-COR model LI-2020 solar tracker.

2.2.4 Cloud Base Height

The Visalia CT 12K ceilometer was used to continuously monitor the height of the cloud base. A maximum height of 3657 m (12,000 feet) can be measured. The ceilometer measures the travel time of a series of short GaAs semiconductor laser pulses to the cloud and back. It can be used to monitor several cloud layer heights. The ceilometer will operate between -50° and 50°C and between 0 and 100% relative humidity. It has an internal sampling rate of 10 MHz to achieve 15 m (50 ft) resolution. Accuracy is within 100 feet or 5% whichever is greater.

2.3 Rawinsonde Station

The rawinsonde data was obtained by using a cross-chain Loran atmospheric sounding system (CLASS). As described by Schubert, *et al.* (1987), CLASS is a portable upper air sounding system contained in a towable trailer. In the trailer are a balloon inflation and launch apparatus, an electronics rack for the reception of the sonde radio frequency (RF) signals, and a desktop computer. A 3 meter tower is located close to the trailer and contains an antenna, preamplifier and surface weather station. The tower consists of two 400 MHz RF antennas, an antenna rotor, an antenna switch, a 400 MHz preamp, and a crossarm which holds the components of the surface weather station. The 400 MHz RF signal from the RS-80L radiosonde is received by the tower antenna and fed to a 500 kHz band width FM receiver manufactured by Communitronics Ltd. Signal outputs are provided for the 7-10 kHz thermodynamic frequencies and the 100 kHz Loran-C frequencies.

The thermodynamic frequencies are processed into units of pressure, temperature, and humidity by a Vaisala PP-11 PTU processor. Here the data is displayed and also sent to an RS-232 serial data port for computer access. The Loran-C frequencies are processed by elements of an aircraft Loran-C navigator which has been modified for use by CLASS. The navigator is an ANI-7000 by Advanced Navigation Inc. It can track as many as eight Loran stations at one time. A 200 gram balloon was used for all the rawinsonde flights from San Nicolas Island.

Chapter 3

DATA DESCRIPTION

3.1 Raw Data

Campbell Scientific Data Loggers (model 21X) collected the data and saved it on cassette tape. The data were later transferred to streaming tape. The data loggers converted much of the data from Volts to the engineering units (°C, W/m^2, etc.). To use the raw data, one must move the data from streaming tape to disk with the program, SYTOS, from Sytron Corporation. The data then can be placed in a desired format by using the Campbell Scientific program, SPLIT. SPLIT will also remove any bad data points. The format of the data on the tapes is nn±dddddss, where nn is a two digit variable index (01, 02,...,99), ± is a plus or a minus sign, ddddd is a five digit real number, and ss is two spaces. This takes up ten spaces, allowing for eight data variables per 80 character line.

There were three data loggers on the balloon platform: one for the basic meteorological data, another for the radiometric data, and the other for the FSSP data. The list of data variables can be found in Tables 3.1, 3.2, and 3.3. Data were saved every 4 seconds for the meteorological data, every 4, 7, or 8 seconds for the radiometric data (depending on the flight), and every 5 seconds for the FSSP data. (Note the wind speed data is with the radiometric data.)

Another data logger collected the surface data from the instruments on the "H-Frame". The data variable list is found in Table 3.4. Note that there are four separate identification numbers in the data. This is to allow SPLIT to pull out a subset of the data. The data were sampled every 5 seconds and saved every 10 minutes.

The MFOV stored its data on cassette tape in the format (2F5.0,20F5.3,F5.0). Table 3.5 gives the description of the variables. Data were saved every 10 minutes.

The ceilometer data was collected on an IBM PC XT. For more information about the ceilometer data see Operation of a Ceilometer During the FIRE Marine Stratocumulus Experiment (Schubert, *et al.*, 1987).

The data from the CLASS rawinsonde system is stored on high density PC floppy disks. Each data file consists of a 7 line header followed by the data records. All records are free format comma delimited ASCII. The CLASS sounding files consist of data collected every 3.3 seconds and data collected every 10 seconds. The data collected every 10 seconds also has wind data. The data files are named using the launched time as a file name and an .SNI extension for the data collected every 10 seconds and an .RAW (or .RW1) extension for the data collected every 3.3 seconds (e.g. the 10 second data file of the 01:12 GMT flight on June 30 is named 06300112.SNI). The format of the files of 10 second data are found in Table 3.6. The quality numbers found in Table 3.6 are variances computed from a running average. It should be noted that the longitude and latitude are computed in different ways depending on signal quality, and thus they may have significant discontinuities. The 3.3 second data has the same format except without the wind and quality data. Appendix B contains a summary of the available rawinsonde flights.

Table 3.1: Variables from the balloon meteorological data logger. Output was every 4 seconds.

INDEX	NAME	DESCRIPTION
1	ID	Identification number: 0138
2	JD	Julian Day
3	HHMM	Hours and minutes on a 24 hour clock (GMT)
4	SEC	Seconds
5	WIND DIR	Wind direction relative to the platform (± 177.5°)
6	PITCH	Platform pitch (± 45°)
7	ROLL	Platform roll (± 45°)
8	PSY1 DRY	Thermistor Psychrometer dry bulb output (mV)
9	PSY1 DT	Thermistor Psychrometer dry minus wet bulb output (mV)
10	BATT VOLT	Platform battery voltage (V)
11	BATT AMPS	Platform battery current-NOT USED
12	PANEL TMP	Internal CR-21X temperature
13	PSY2 DRY	Thermocouple psychrometer dry bulb temperature (°C)
14	PSY2 WET	Thermocouple psychrometer wet bulb temperature (°C)
15	BOX1 TEMP	Data logger electronics box internal temperature (°C)
16	BOX2 TEMP	VCR elctronics box internal temperature (°C)
17	AIR TEMP	AM-32 Mux. temperature (°C)
18	RH	Data logger electronics box internal relative humidity (percent)
19	COMPASS1	Platform direction compass #1 (± 180°)
20	COMPASS2	Platform direction compass #2 (± 180°)
21	PRESS-FQ	Digiquartz pressure transducer output (kHz)
22	TEMP-FQ	Digiquartz pressure transducer internal temperature output (kHz)
23	PRESS-MB	Pressure output (mb)
24	TEMP-DEG C	Presure transducer internal temperature (°C)
25	VCR FLAG	VCR record on/off flag
26	VCR TIME	VCR recording time (hours)

Table 3.2: Variables from the balloon radiation data logger. Output was every 4, 7, or 8 seconds.

INDEX	NAME	DESCRIPTION
1	ID	Identification number: 0207
2	JD	Julian Day
3	HHMM	Hours and minutes on a 24 hour clock (GMT)
4	SEC	Seconds
5	UPBUG1	Upfacing bugeye channel 1 (mV)
6	UPBUG2	Upfacing bugeye channel 2 (mV)
7	UPBUG3	Upfacing bugeye channel 3 (mV)
8	UPBUG4	Upfacing bugeye channel 4 (mV)
9	UPBUG5	Upfacing bugeye channel 5 (mV)
10	UPBUG6	Upfacing bugeye channel 6 (mV)
11	UPBUG7	Upfacing bugeye channel 7 (mV)
12	UPBUG8	Upfacing bugeye channel 8 (mV)
13	UPBUG9	Upfacing bugeye channel 9 (mV)
14	UPBUG10	Upfacing bugeye channel 10 (mV)
15	UPBUG11	Upfacing bugeye channel 11 (mV)
16	UPBUG12	Upfacing bugeye channel 12 (mV)
17	UPBUG13	Upfacing bugeye channel 13 (mV)
18	DNBUG1	Downfacing bugeye channel 1 (mV)
19	DNBUG2	Downfacing bugeye channel 2 (mV)
20	DNBUG3	Downfacing bugeye channel 3 (mV)
21	DNBUG4	Downfacing bugeye channel 4 (mV)
22	DNBUG5	Downfacing bugeye channel 5 (mV)
23	DNBUG6	Downfacing bugeye channel 6 (mV)
24	DNBUG7	Downfacing bugeye channel 7 (mV)
25	DNBUG8	Downfacing bugeye channel 8 (mV)
26	DNBUG9	Downfacing bugeye channel 9 (mV)
27	DNBUG10	Downfacing bugeye channel 10 (mV)
28	DNBUG11	Downfacing bugeye channel 11 (mV)
29	DNBUG12	Downfacing bugeye channel 12 (mV)
30	DNBUG13	Downfacing bugeye channel 13 (mV)

Table 3.2: Continued.

INDEX	NAME	DESCRIPTION
31	FIRUP	Far IR upfacing pyrgeometer (mV)
32	FIRDN	Far IR downfacing pyrgeometer (mV)
33	TOTUP	Total pyranometer upfacing (W/m^2)
34	NIRUP	Near IR upfacing pyranometer (W/m^2)
35	TOTDN	Total pyranometer downfacing (W/m^2)
36	NIRDN	Near IR downfacing pyranometer (W/m^2)
37	DT-UP	Dome temperature of upfacing pyrgeometer (V)
38	DT-DN	Dome temperature of downfacing pyrgeometer (V)
39	ST-UP	Sink temperature of upfacing pyrgeometer (V)
40	ST-DN	Sink temperature of downfacing pyrgeometer (V)
41	FUNK	Funk net radiometer (mV)
42	BUGETTE	Upfacing photodiode (mV)
43	LU	Longwave upfacing pyrgeometer (W/m^2)
44	LD	Longwave downfacing pyrgeometer (W/m^2)
45	WIND SP	Wind speed (m/s)

Table 3.3: Variables from the balloon FSSP data logger. Output was every 5 seconds.

INDEX	NAME	DESCRIPTION
1	ID	Identification number: 0102
2	JD	Julian Day
3	HHMM	Hours and minutes on a 24 hour clock (GMT)
4	SEC	Seconds
5	BIN 0	FSSP size channel 0 number of particles
6	BIN 1	FSSP size channel 1 number of particles
7	BIN 2	FSSP size channel 2 number of particles
8	BIN 3	FSSP size channel 3 number of particles
9	BIN 4	FSSP size channel 4 number of particles
10	BIN 5	FSSP size channel 5 number of particles
11	BIN 6	FSSP size channel 6 number of particles
12	BIN 7	FSSP size channel 7 number of particles
13	BIN 8	FSSP size channel 8 number of particles
14	BIN 9	FSSP size channel 9 number of particles
15	BIN 10	FSSP size channel 10 number of particles
16	BIN 11	FSSP size channel 11 number of particles
17	BIN 12	FSSP size channel 12 number of particles
18	BIN 13	FSSP size channel 13 number of particles
19	BIN 14	FSSP size channel 14 number of particles
20	BIN 15	FSSP size channel 15 number of particles

INDEX	NAME	DESCRIPTION
21	STROBES	Number of real particles counted during the scan
22	TOT STBS	Total number of particles (real or false) sensed by the FSSP
23	RANGE	Range codes to determine the range of particles for the FSSP to sense (00 = 2 - 47 μm, 01 = 2 - 32 μm, 02 = 1 - 16 μm, 03 = 0.5 - 8 μm)

Table 3.4: Variables from the surface "H-Frame" data loggers. Data were sampled every 5 seconds with output being sent every 10 minutes.

INDEX	NAME	DESCRIPTION
		— first section —
1	ID	Identification number: 0103
2	JD	Julian Day
3	HHMM	Hours and minutes on a 24 hour clock (GMT)
4	AV WIND SP	Average wind speed (m/s)
5	MN WVMAG	Mean wind vector magnitude (m/s)
6	MN WIND DIR	Mean wind direction (0 to 359°)
7	SD WIND DIR	Standard deviation of Wind Direction
		— second section —
1	ID	Identification number: 0208
2	JD	Julian Day
3	HHMM	Hours and minutes on a 24 hour clock (GMT)
4	AV TOT-UP V	Average total pyranometer upfacing (mV)
5	AV NIR-UP V	Average near IR pyranometer upfacing (mV)
6	AV TOT-UP	Average total pyranometer upfacing (W/m^2)
7	AV NIR-UP	Average near IR pyranometer upfacing (W/m^2)
8	AV FIR-UP	Average longwave pyrgeometer upfacing (mV)
9	AV SKT-UP	Average sink temperature of pyranometer upfacing (V)
10	AV DMT-UP	Average dome temperature of pyranometer upfacing (V)
11	AV LU	Average longwave pyrgeometer upfacing (W/m^2)
12	AV SKT-UP K	Average sink temperature of pyranometer upfacing (°K)
13	AV DMT-UP K	Average dome temperature of pyranometer upfacing (°K)

Table 3.4: Continued.

INDEX	NAME	DESCRIPTION
		— third section —
1	ID	Identification number: 0217
2	AV TOT-UP V	Standard Deviation of total pyranometer upfacing (mV)
3	AV NIR-UP V	Standard Deviation of near IR pyranometer upfacing (mV)
4	AV TOT-UP	Standard Deviation of total pyranometer upfacing (W/m^2)
5	AV NIR-UP	Standard Deviation of near IR pyranometer upfacing (W/m^2)
6	AV FIR-UP	Standard Deviation of longwave pyrgeometer upfacing (mV)
7	AV SKT-UP	Standard Deviation of the sink temperature of pyranometer upfacing (V)
8	AV DMT-UP	Standard Deviation of the dome temperature of pyranometer upfacing (V)
9	AV LU	Standard Deviation longwave pyrgeometer upfacing (W/m^2)
		— fourth section —
1	ID	Identification number: 0224
2	JD	Julian Day
3	HHMM	Hours and minutes on a 24 hour clock (GMT)
4	AV AT	Average air temperature (°C)
5	AV R/H	Average relative humidity (percent)
6	SD AT	Standard deviation of air temperature (°C)
7	SD R/H	Standard deviation of relative humidity (percent)
8	AV SPAT	Average air temperature (°C)–Spare

3.2 Processed Balloon Data

The post-experiment processing of the balloon data set consisted of normalizing the bugeye diode outputs to a relative bugette voltage, recalculating the longwave irradiances calculating the microphysical cloud parameters from FSSP data, and finding the absolute wind direction (using platform direction and the relative wind direction). A cubic spline routine was then used to interpolate the balloon data to the same times with a time interval of five seconds between data points. Table 3.7 lists

Table 3.5: Variables from the Multi-Field Of View. Output was every 10 minutes.

INDEX	VARIABLE DESCRIPTION
1	Julian Day
2	Hours and minutes on a 24 hour clock (GMT)
3	Average of 28° field of view (V)
4	Average of 20° field of view (V)
5	Average of 10° field of view (V)
6	Average of 5° field of view (V)
7	Average of 2° field of view (V)
8	Standard deviation of 28° field of view (V)
9	Maximum of 28° field of view (V)
10	Minimum of 28° field of view (V)
11	Standard deviation of 20° field of view (V)
12	Maximum of 20° field of view (V)
13	Minimum of 20° field of view (V)
14	Standard deviation of 10° field of view (V)
15	Maximum of 10° field of view (V)
16	Minimum of 10° field of view (V)
17	Standard deviation of 5° field of view (V)
18	Maximum of 5° field of view (V)
19	Minimum of 5° field of view (V)
20	Standard deviation of 2° field of view (V)
21	Maximum of 2° field of view (V)
22	Minimum of 2° field of view (V)
23	Battery voltage (V)

Table 3.6: Header format and data variables of the CLASS rawinsonde.

The header contains:

Line 1

Field	Description
1	Site (SNI)
2	Year
3	Month and day (mmdd)
4	Time (hhmm in GMT)
5	Site longitude (degrees)
6	Site latitude (degrees)

Line 2

Field	Description
1	Data type (CLASS DATA)
2	Version (78)

Lines 3-6

Operator's comments.

Line 7 (surface observation)

Field	Description
1	Time (seconds)
2	Height (meters)
3	Pressure (millibars)
4	Temperature (°C)
5	Dewpoint temperature (°C)
6	Relative humidity (%)
7	u wind speed (m/s)
8	v wind speed (m/s)

The data records contain:

Field	Description
1	Time (seconds)
2	Height (meters)
3	Pressure (millibars)
4	Temperature (°C)
5	Dewpoint temperature (°C)
6	Relative humidity (%)
7	u wind speed (m/s)
8	v wind speed (m/s)
9	Pressure quality
10	Temperature quality
11	Humidity quality
12	u wind quality
13	v wind quality
14	Longitude (degrees)
15	Latitude (degrees)

the variables included in the processed data set. The format of the processed data set is (4F5.0,F6.0,F5.1,2F6.2,F7.1,27F8.3,6F6.1,F4.0,15F6.3,F6.1,F6.3,2F5.1).

3.2.1 Radiation

The diodes of the bugeye instruments have different sensitivities and dark current biases. Because of this, calibration data were used to normalize each diode to the voltage of the bugette. The normalized voltages can now be compared directly with one another.

The longwave irradiances were recalculated using new calibration data and correct dome and sink temperatures. Albrecht and Cox (1976) describe the data reduction and calibration procedures used.

3.2.2 Wind Direction

The wind direction was found to contain a large number of erroneous data points. The erroneous data points were believed to be the result of the compasses not always latching properly before a compass reading. The following procedure was used to correct the data.

The two compass readings from each data line were compared. If the compass readings differed by more than 15 degrees, that data line was ignored. If the compasses were within 15 degrees of each other, they were averaged and summed with their corresponding relative wind direction reading, yielding an absolute wind direction measurement. The data were then filtered.

In filtering the data, a wind direction data point was compared with the adjacent wind direction data points. If the center wind direction differed from either the previous wind direction or the following wind direction by more than 15 degrees, the center wind direction was removed. If both differences were less than 15 degrees, the center wind direction was kept. This eliminated many of the erroneous peaks in the data. The process was then repeated for each data point through out the data file. The remaining wind directions and their corresponding times were used in a cubic spline interpolation routine to replace the missing wind directions.

3.2.3 Microphysical Data

From the raw FSSP data, droplet size distributions were calculated for each flight. Additional variables, such as the liquid water content (LWC), mean droplet radius (r_m), effective droplet radius (r_e) and number densities (N) were computed from the droplet size distributions.

In order to determine these quantities, several factors were considered. The sampling volume was determined by the depth-of-field of the focused laser beam and the percentage of particles accepted by the velocity averaging circuitry of the probe. The effective cross-sectional area of the laser beam (A_e) was calculated by multiplying the measured cross-section with the ratio between the accepted counts and the total counts.

$$A_e = A \times AC \div TC,$$

where A is the measured cross-section (4.6×10^{-7} m^2), AC the total accepted counts, and TC the total counts (accepted + rejected).

An estimate of the speed of the particles through the sampling volume was made by multiplying the windspeed by the cosine of the angle between the wind and the instrument platform. Thus, the sampling volume is

$$V = A_e v,$$

where v is the true airspeed and the concentration of particles in one channel is

$$n_j = \frac{C_j}{V \delta t},$$

where C_j is the number of droplets counted in the j^{th} channel and δt is the sampling interval (5 seconds). In order to prevent the estimates of the particle concentrations from being erroneously large, the calculations were not made when relative wind direction became large (> 60 °) or the particle speed became small (< 4 m/s).

The total number density is the summation of the particle concentrations in each channel,

$$N = \sum_{j=1}^{15} n_j.$$

The average droplet radius in each channel depended upon the size range set for the instrument. For all research flights, the FSSP probe was set to range 0 (range 0 radii = 1 - 23.5 μm). The radii of the droplets in each channel were assumed to be the midpoint value of each channel. Thus, with the instrument set to range 0, the average droplet radius in each channel was

$$r_j = (3j + 0.5)/2$$

where r_j is expressed in microns. The mean radius of the particles was computed from

$$r_m = \frac{1}{N} \sum_{j=1}^{15} n_j r_j$$

and the effective radius of the particles was calculated from

$$r_e = \frac{\sum_{j=1}^{15} n_j r_j^3}{\sum_{j=1}^{15} n_j r_j^2}.$$

The liquid water content was calculated from

$$LWC = \frac{4}{3} \pi \rho_L \sum_{j=1}^{15} n_j r_j^3,$$

where ρ_L is the density of water.

The wind speed and wind direction data were collected at different data collection rates than the FSSP data. In order to synchronize the data, the wind direction and wind speed data were linearly interpolated to the times of the FSSP data. The droplet size distributions and liquid water contents were calculated for five second time intervals.

The FSSP probe had several problems which limited the performance of the instrument. During several flights, the least significant bit was missing from the output of the pulse height analyzer. The loss of this bit results in the information from each pair of bins (0–1, 2–3, 4–5,...) being placed in the lower bin, and consequently a loss of some resolution. The FSSP data from Flight 8 (13 July 1987) and Flight 9 (13-14 July 1987) were considered to be unusable.

The droplet size distributions were normalized and stored in either eight or fifteen size ranges, depending on the resolution of the raw FSSP data. (Variable BIN gives the number of bins used.) The droplet concentrations for each bin can be found by multiplying the normalized concentration by the total number density.

Table 3.7: Processed Balloon Data.

INDEX	NAME	DESCRIPTION
1	JD	Julian Day
2	HOUR	Hours (GMT)
3	MINUTE	Minutes
4	SEC	Seconds
5	WIND DIR	Wind direction
6	WIND SP	Wind speed (m/s)
7	PSY DRY	Thermocouple psychrometer dry bulb temperature (°C)
8	PSY WET	Thermocouple psychrometer wet bulb temperature (°C)
9	PRESS-MB	Pressure output (mb)
10	UPBUG1	Upfacing bugeye channel 1 (mV)
11	UPBUG2	Upfacing bugeye channel 2 (mV)
12	UPBUG3	Upfacing bugeye channel 3 (mV)
13	UPBUG4	Upfacing bugeye channel 4 (mV)
14	UPBUG5	Upfacing bugeye channel 5 (mV)
15	UPBUG6	Upfacing bugeye channel 6 (mV)
16	UPBUG7	Upfacing bugeye channel 7 (mV)
17	UPBUG8	Upfacing bugeye channel 8 (mV)
18	UPBUG9	Upfacing bugeye channel 9 (mV)
19	UPBUG10	Upfacing bugeye channel 10 (mV)
20	UPBUG11	Upfacing bugeye channel 11 (mV)
21	UPBUG12	Upfacing bugeye channel 12 (mV)
22	UPBUG13	Upfacing bugeye channel 13 (mV)
23	DNBUG1	Downfacing bugeye channel 1 (mV)
24	DNBUG2	Downfacing bugeye channel 2 (mV)
25	DNBUG3	Downfacing bugeye channel 3 (mV)
26	DNBUG4	Downfacing bugeye channel 4 (mV)
27	DNBUG5	Downfacing bugeye channel 5 (mV)
28	DNBUG6	Downfacing bugeye channel 6 (mV)
29	DNBUG7	Downfacing bugeye channel 7 (mV)
30	DNBUG8	Downfacing bugeye channel 8 (mV)

Table 3.7: Continued.

INDEX	NAME	DESCRIPTION
31	DNBUG9	Downfacing bugeye channel 9 (mV)
32	DNBUG10	Downfacing bugeye channel 10 (mV)
33	DNBUG11	Downfacing bugeye channel 11 (mV)
34	DNBUG12	Downfacing bugeye channel 12 (mV)
35	DNBUG13	Downfacing bugeye channel 13 (mV)
36	BUGETTE	Upfacing photodiode (mV)
37	TOTUP	Total pyranometer upfacing (W/m^2)
38	NIRUP	Near IR upfacing pyranometer (W/m^2)
39	TOTDN	Total pyranometer downfacing (W/m^2)
40	NIRDN	Near IR downfacing pyranometer (W/m^2)
41	LONUP	Longwave upfacing pyrgeometer (W/m^2)
42	LONDN	Longwave downfacing pyrgeometer (W/m^2)
43	BIN	Number of bins used (Resolution)
44	NDSD1	Normalized droplet size distribution bin 1
45	NDSD2	Normalized droplet size distribution bin 2
46	NDSD3	Normalized droplet size distribution bin 3
47	NDSD4	Normalized droplet size distribution bin 4
48	NDSD5	Normalized droplet size distribution bin 5
49	NDSD6	Normalized droplet size distribution bin 6
50	NDSD7	Normalized droplet size distribution bin 7
51	NDSD8	Normalized droplet size distribution bin 8
52	NDSD9	Normalized droplet size distribution bin 9
53	NDSD10	Normalized droplet size distribution bin 10
54	NDSD11	Normalized droplet size distribution bin 11
55	NDSD12	Normalized droplet size distribution bin 12
56	NDSD13	Normalized droplet size distribution bin 13
57	NDSD14	Normalized droplet size distribution bin 14
58	NDSD15	Normalized droplet size distribution bin 15
59	ND	Total number density (cm^{-1})
60	LWC	Liquid water content (g/m^3)
61	RE	Effective droplet radius (μm)
62	RM	Mean droplet radius (μm)

REFERENCES

Albrecht, B., and S.K. Cox, 1976: Pyrgeometer data reduction and calibration procedures. Atmos. Sci. Paper No. 251, Colorado State University, Ft. Collins, 48 pp.

Cox, S.K., D.S. McDougal, D.A. Randall, and R.A. Schiffer, 1987: FIRE–the first ISCCP regional experiment. *Bull. Amer. Meteor. Soc.*, **68**, 114-118.

Davis, J.M., C. Vogel, and S.K. Cox, 1982: Multidirectional photodiode array for measurement of solar radiances. *Rev. Sci. Instrum.*, **53**, 667-673.

Randall, D.A., J.A. Coakley, Jr., C.W. Fairall, R.A. Kropfli, and D.H. Lenschow, 1984: Outlook for reseach on subtropical marine stratiform clouds. *Bull. Amer. Meteor. Soc.*, **65**, 1290-1301.

Schubert, W.H., P.E. Ciesielski, T.B. McKee, J.D. Kleist, S.K. Cox, C.M. Johnson-Pasqua, and W.L. Smith, 1987: Analysis of boundary layer sounding data from the FIRE Marine Stratocumulus Project: FIRE volume 2. Atmos. Sci. Paper No. 419, Colorado State University, Ft. Collins, 101 pp.

Schubert, W.H., S.K. Cox, P.E. Ciesielski, and C.M. Johnson- Pasqua, 1987: Operation of a ceilometer during the FIRE marine stratocumulus experiment: FIRE volume 3. Atmos. Sci. Paper No. 420, Colorado State University, Ft. Collins, 34 pp.

Appendix A

CSU TETHERED BALLOON RESEARCH SUMMARY

5 July 1987 First Flight 2 hours long

This was a test flight. (The flight was delayed many days because strong winds prevented the balloon from being inflated.)

PROBLEMS: FSSP data was missing its least significant bit.

7 July 1987 Second Flight 9 hours 52 minutes long

The balloon was launched at 07:45 PDT. The Britsh Meteorology Office (BMO) attached six packages as the balloon was taken to 2400 ft. BMO did four 68 minute runs while the CSU package was above cloud. At 13:25 PDT CSU begins two soundings with 5 minute legs at each 300 ft level.

PROBLEMS: FSSP data was missing its least significant bit. Wet bulb wicks appeared to have a problem. The bugeye gain might have been set too high.

8 July 1987 Third Flight 6.5 hours long

The balloon launch was at 07:30 PDT. Four BMO packages were deployed at 100 ft intervals just below the CSU package. Four 20 constant level runs were done with the packages near cloud top (about 935 mb). The balloon was brought down in 200 ft steps with 20 minutes at each level.

PROBLEMS: FSSP data was missing its least significant bit. The bugeye gain was too high.

9 July 1987 Fourth Flight 4.0 hours long

The balloon was launched at 08:31 PDT and went into a very deep cloud with a top near 950 meters. It was drizzling. The flight was shortened because BMO could not get its highest package above cloud top.

PROBLEMS: FSSP data was missing its least significant bit. The downward-looking bugeye was full of water. The thermistor psychrometer was inoperative due to a broken wire.

10 July 1987 Fifth Flight 10.0 hours long

The balloon launch was at 08:34 PDT into a very deep boundary layer (about 1000 m). Because of the deep boundary layer BMO packages were not placed on the balloon. The CSU package stepped upward in 300 ft intervals with 20 minutes at each level. Several 15 minute legs at 50 ft intervals were performed near cloud top on the descent.

PROBLEMS: Downward-looking bugeye channel #13 was bad.

11 July 1987 Sixth Flight 9.5 hours long

The balloon was launched at 13:35 PDT for an afternoon and evening flight. BMO deployed six packages, but took off the lowest one because there was some difficulty in getting the balloon above cloud top. BMO did two 64 minute runs and after that CSU steps down with eleven 20 minute legs.

PROBLEMS: Downward-looking bugeye channel #13 was bad.

12 July 1987 Seventh Flight 1.0 hour long

The balloon launch was at 03:40 PDT, but at about 930 mb slack developed in the cable. The balloon, carrying the CSU and four BMO packages, was brought down quickly. It was decided that the balloon could no longer lift both the CSU and BMO packages.

PROBLEMS: The balloon had little lift.

13 July 1987 Eighth Flight 11.5 hours long

The balloon was launched at 09:20 PDT with only the CSU package. Cloud top was near 960 mb. Sixteen 20 minute legs were run in the cloud layer and nine more in the subcloud layer.

PROBLEMS: FSSP was missing every other pair of channels.

13-14 July 1987 Ninth Flight 6.5 hours long

The balloon was launched at 21:45 PDT with the CSU package for a night mission. A low cloud top still persisted. Twenty constant level legs were performed in the boundary layer.

PROBLEMS: FSSP shifted its output to the lower end of the spectrum.

Appendix B

CLASS RAWINSONDE FLIGHT SUMMARY

Flight Number	Date	Begin Time(GMT)	End Time(GMT)	Maximum Altitude (km)	Quality Wind	Quality Temp/Hum
0	June 29	01:12:03	01:28:28	2.0	poor	poor
1	June 30	11:55:00	13:37:39	21.5	fair	good
2	June 30	23:51:28	01:41:48	24.1	fair	good
3	July 1	12:16:51	13:28:37	18.7	fair	good
4	July 1	20:05:16	20:58:01	13.0	poor	good
5	July 1	23:11:39	00:15:45	16.6	fair	good
6	July 2	12:—:—	———	—.–	poor	poor
7	July 2	17:50:00	———	20.7	fair	good
8	July 2	22:53:39	23:52:14	16.8	good	good
9	July 3	12:08:46	13:24:00	39.4	fair	good
10	July 3	18:08:34	19:24:02	21.1	fair	good
11	July 4	00:36:55	02:00:34	7.1	good	good
12	July 4	12:15:10	13:38:41	21.6	poor	good
13	July 5	00:34:11	01:48:03	19.7	fair	good
14	July 5	11:58:40	13:07:09	18.9	good	good
15	July 6	01:45:48	03:01:10	19.5	poor	good
16	July 6	12:14:14	13:32:45	18.8	fair	good
17	July 6	16:07:18	17:35:41	21.0	good	good
18	July 6	23:50:14	00:15:17	—.–	poor	poor
19	July 7	11:19:34	12:33:38	19.9	fair	good
20	July 8	00:11:58	01:21:07	20.0	poor	good
21	July 8	12:11:57	13:14:15	18.8	poor	good
22	July 9	11:54:19	12:53:09	17.9	fair	good
23	July 9	18:14:58	19:27:51	20.0	poor	good
24	July 10	01:15:14	02:39:12	20.8	fair	good
25	July 10	12:22:51	13:11:10	9.6	good	good
26	July 10	15:50:39	17:00:19	19.6	good	good
27	July 10	18:00:56	19:37:41	22.0	fair	good
28	July 10	20:06:53	21:14:59	20.4	good	good
29	July 10	21:59:53	23:05:08	20.0	fair	good

Flight Number	Date	Begin Time(GMT)	End Time(GMT)	Maximum Altitude (km)	Quality Wind	Quality Temp/Hum
30	July 11	00:05:46	01:27:35	20.8	poor	good
31	July 11	02:00:25	03:12:40	20.1	poor	good
32	July 11	03:53:52	05:16:38	21.1	fair	good
33	July 11	06:16:41	07:26:30	19.5	poor	good
34	July 11	09:51:50	11:06:57	20.2	poor	good
35	July 11	12:12:45	13:27:27	19.2	poor	good
36	July 11	14:10:50	15:21:15	20.6	fair	fair
37	July 11	18:08:30	19:40:40	22.1	fair	good
38	July 11	22:08:06	23:33:40	21.5	poor	fair
39	July 11	23:49:42	01:21:01	22.1	fair	fair
40	July 12	01:54:12	03:12:19	20.8	poor	good
41	July 12	06:10:54	07:32:45	19.5	good	good
42	July 12	12:34:09	14:34:14	21.5	fair	good
43	July 12	15:10:57	16:34:09	21.3	poor	good
44	July 12	10:05:10	11:32:05	19.7	good	good
45	July 12	17:55:31	———	22.0	good	good
46	July 13	00:05:41	01:27:34	20.4	fair	good
47	July 13	11:54:13	12:58:54	18.2	fair	good
48	July 13	21:20:07	22:50:25	22.8	fair	good
49	July 14	00:14:06	01:30:02	19.3	fair	good
50	July 14	11:58:11	13:02:58	20.0	poor	good
51	July 15	00:15:59	01:09:54	14.9	fair	fair
52	July 15	12:00:54	13:12:57	16.2	poor	fair
53	July 15	17:03:55	18:21:47	20.2	good	good
54	July 15	19:35:49	20:43:39	18.6	poor	good
55	July 16	00:11:18	01:37:34	21.5	good	good
56	July 16	11:39:09	13:31:11	24.2	fair	good
57	July 16	16:00:08	17:17:54	21.6	fair	good
58	July 16	20:04:08	21:29:00	23.6	poor	good
59	July 16	23:42:05	00:59:44	21.3	poor	good
60	July 17	12:06:30	13:31:06	21.0	fair	good
61	July 17	15:58:23	17:09:44	20.7	poor	good
62	July 17	20:02:15	21:24:24	22.0	fair	good
63	July 18	00:20:31	01:32:37	20.6	poor	good
64	July 18	12:06:33	13:43:42	21.7	poor	good
65	July 18	15:57:44	17:07:40	20.3	good	good
66	July 18	19:51:33	21:27:11	22.0	fair	good
67	July 19	00:19:47	02:08:49	24.0	good	good
68	July 19	12:01:01	13:25:58	21.6	fair	good
69	July 19	16:08:32	17:48:35	23.1	fair	good
70	July 19	20:15:35	21:28:17	21.1	poor	good